Optical design of an autoguider for the Hanle Observatory

Revised for 2nd commissioning run

Copenhagen University Observatory

August 2005

Contents

1 Introduction

This report describes the optics of the autoguider for the Hanle Observatory, currently being built by Copenhagen University Observatory (CUO).

The basic design idea is to use a fixed guide field, large enough to ensure that a suitable guide star will be available. The field position and optics layout is constrained by the geometry of the adapter cube in which it is to be placed and the requirement that the science beam must not be vignetted.

2 Limiting guide star magnitude

The prediction of the faintest useable guide stars for the camera is based on the following: The camera is equipped with a KAF-3200E CCD, which is a front side illuminated detector with a relatively high QE, peaking around 65%. An even more efficient version with micro-lenses is available, but this is not evaluated. The guide frequency assumed here is 1Hz, although image rates in the 0.1Hz to 4Hz range are expected to be available. 1Hz seems like a good compromise between sky coverage and response time. The camera is assumed to have a read-out noise of about 15e$^-$, and a dark current of about 7.5e$^-$/pix/sec at 19°C. The pixel scale is 0.33 arcsec/pixel. Binning is not used. A spot size contribution of 0.85 arcseconds FWHM from the optics is included.

For reference star signal, V-band ALFOSC data from the 2.56m Nordic Optical Telescope is used. This includes telesope efficiency, and the throughput of the focal reducer is expected to be similar to ALFOSC. The count rate is scaled according to the ratio of the collecting area of the Nordic and Hanle telescopes.

The guider uses the 550nm to 800nm range, i.e. the V, R and some of the I band. A somewhat pessimistic extrapolation of the data is used here, assuming the same star and sky background flux at the longer wavelengths as for the V band, while the conditions in the red in reality are expected to be more favourable. Sky backgrounds for dark time (m$_V$=21.8/"^{2}), full moon (m$_V$=18.5/"^{2}) [TNG WWW] and a guess of the sky brightness with cirrus at full moon (m$_V$=16/"^{2}) are investigated in different seeing conditions. The required signal to noise ratio is derived from experience with the HiRAC fast guider, where a S/N $\geq$ 4 per quadrant was required. An algoritm determining the centroid in a small image will require a better signal, though.

The graph in figure 1 displays the results. It appears that stars of m$_V$=16 will allow guiding in quite adverse conditions and a m$_V$=17 star will commonly be useable.

3 Sky coverage

The probability of finding a star suitable for guiding near the galactic north pole is plotted in figure 2 for a field size of 97 square arcminutes. Star densities are from [Allen 73]. In the previous section it was concluded that a guide star of m$_V$ = 16 would be sufficient. A field of 97 square arcminutes will give a 99% probability of finding a star of m$_V$ = 16 or brighter, even at the galactic pole.

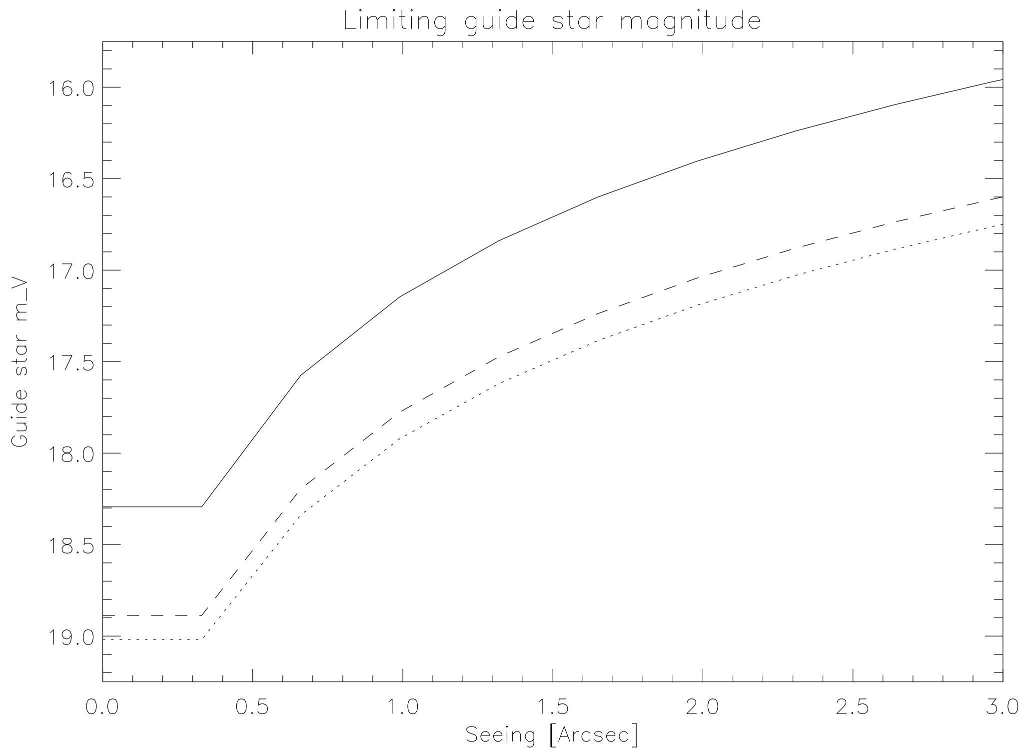

Figure 1: Limiting guide star magnitudes for 1 sec exposures in different seeing conditions and for three sky backgrounds: Dotted graph is for dark time, dashed line for full moon and full drawn line is an estimate for some cirrus during full moon.

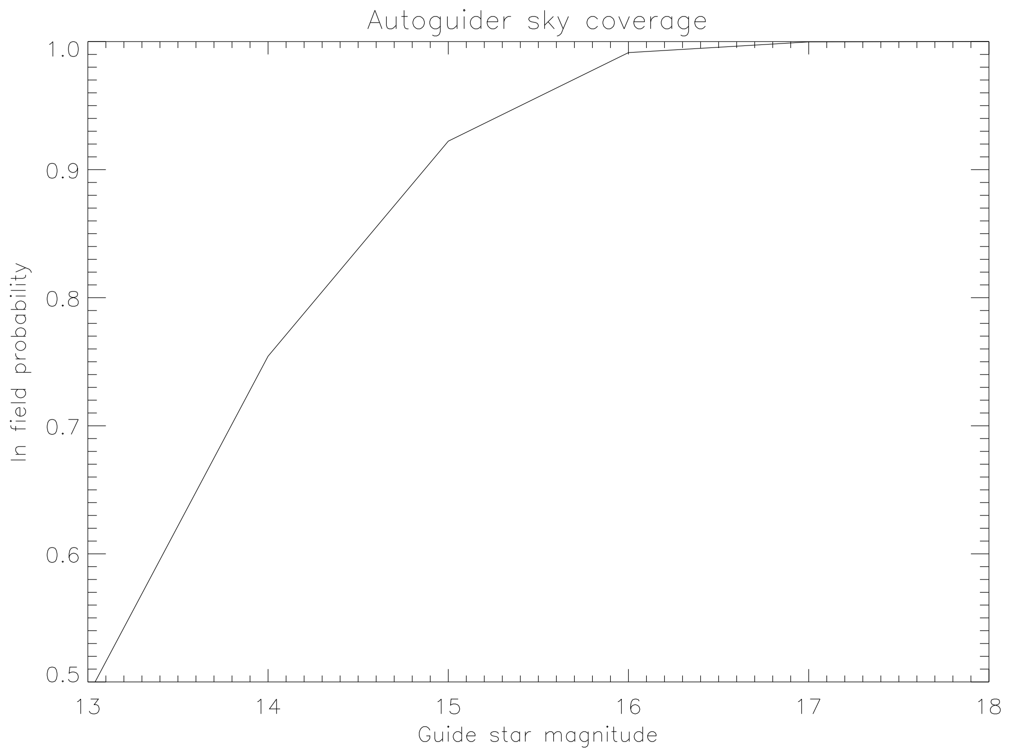

Figure 2: Probability of finding a star of given magnitude near the galactic north pole, within a field of 97 square arcminutes.

4 Field of view for guiding

The first component of the autoguider is a pick-up mirror placed at an angle of 45 degrees to the optical axis, to direct the guide field to the horisontal guide optics. The mirror is located 230mm above telescope focus and has dimensions of 100mm x 90mm, or 71mm x 90mm in 45 degrees projection. A field of 8.1 x 12.0 arcminutes = 97 square arcminutes is reflected towards the autoguider optics.

The centre of the guide field is 18.4 arcminutes off-axis. This distance was chosen as a compromise between mechanial constraints and sources of vignetting.

The lower part of the pick-up mirror is 195mm above focus. At this height, rays reaching the extreme corner of the HFOSC field passes up to 60mm from the optical axis. The edge of the mirror is 57.5mm from the axis, which means that one corner of the HFOSC field will be vignetted, although very slight.

The field for guiding is somewhat vignetted, as illustrated by the map in figure 3. The partially blocked pupil is shown for 12 field positions at the location of the pick-up mirror.

A permanent source of vignetting is a plate immediately above the tertiary mirror, supporting the rotating spider. This has a rectangular opening of 11 x 23 cm on the side of the optical axis where the pick-up mirror is located. As the mirror is rotated 45 degrees relatively to the opening, the two corners of the field away from the axis are partially blocked. This can be seen in the upper and lower corners to the right in figure 3. In the strongest affected field position, the vignetting is about 20%.

With the tertiary mirror in position to feed instruments on the side of the adapter cube, a slight vignetting of the guide field occurs. This is seen in figure 3 as obscuration of the leftmost field spots, with a light loss of about 30% in worst case. Also in the top left corner, obscuration from the mirror arm is seen, causing a 35% loss of light.

Using a partially obscured guide star should not create any difficulties when auto-focus is not used, but the stars must be brighter and hence the sky coverage is degraded.

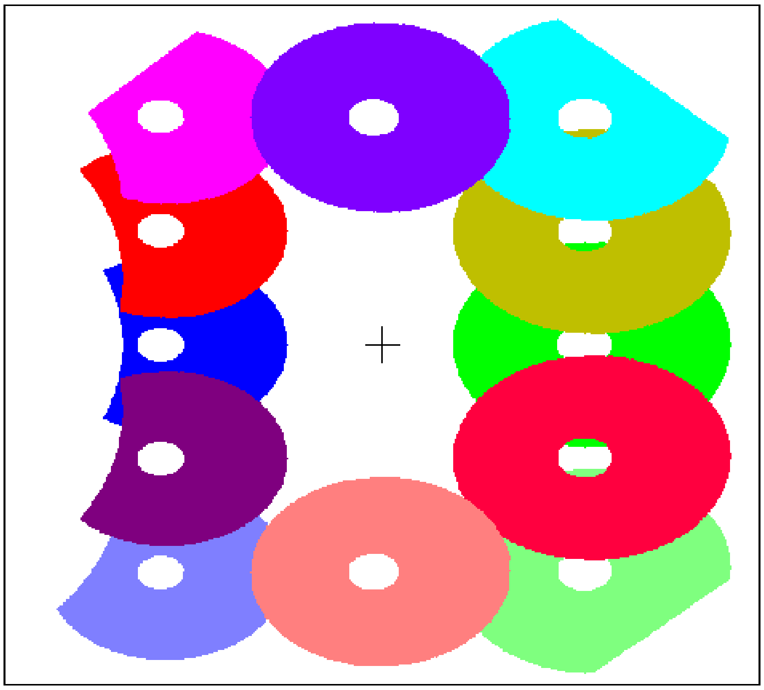

Figure 3: Vignetting map for 12 field positions at the location of the pick-up mirror. The positions are along the edge of the assigned field, as there is no vignetting in the central part. The box outlines the 100x90mm mirror. The optical axis is towards the left.

5 Focal reducer guider lay-out

The guider consists of a pick-up mirror, a folding mirror, a collimator and a camera with a KAF-3200 CCD. The required reduction in image scale is 4.3, resulting in a final focal ratio of 2.1.

The general layout is shown in figure 4. The collimator contains two elements, with the first necessarily being quite large with a diameter of 112mm. The camera is made from a doublet and three singlets.

The starting point for the design was a focal reducer camera designed by Michael I. Andersen, AIP. Also intended for off-axis imaging, this included a cylindric element and a tilted detector plane, in order to partially correct the field aberrations of a telescope. In the current design, however, all lens surfaces are spherical, and off-axis correction is accomplished by de-centering a number of the components without introducing tilt.

In the collimated beam, a filter allows passage of wavelengths from 550nm to 800nm. Outside this range, the optical quality rapidly degrades, so operation without the filter will not be useful.

As an option, a focus pyramid can be inserted in the collimated beam, producing four guide star images. This can provide auto-focus for the telescope, but requires guide stars about one magnitude brighter. In view of the quite strong vignetting of the guide field, it is perhaps not feasible to properly calibrate the autofocus signal.

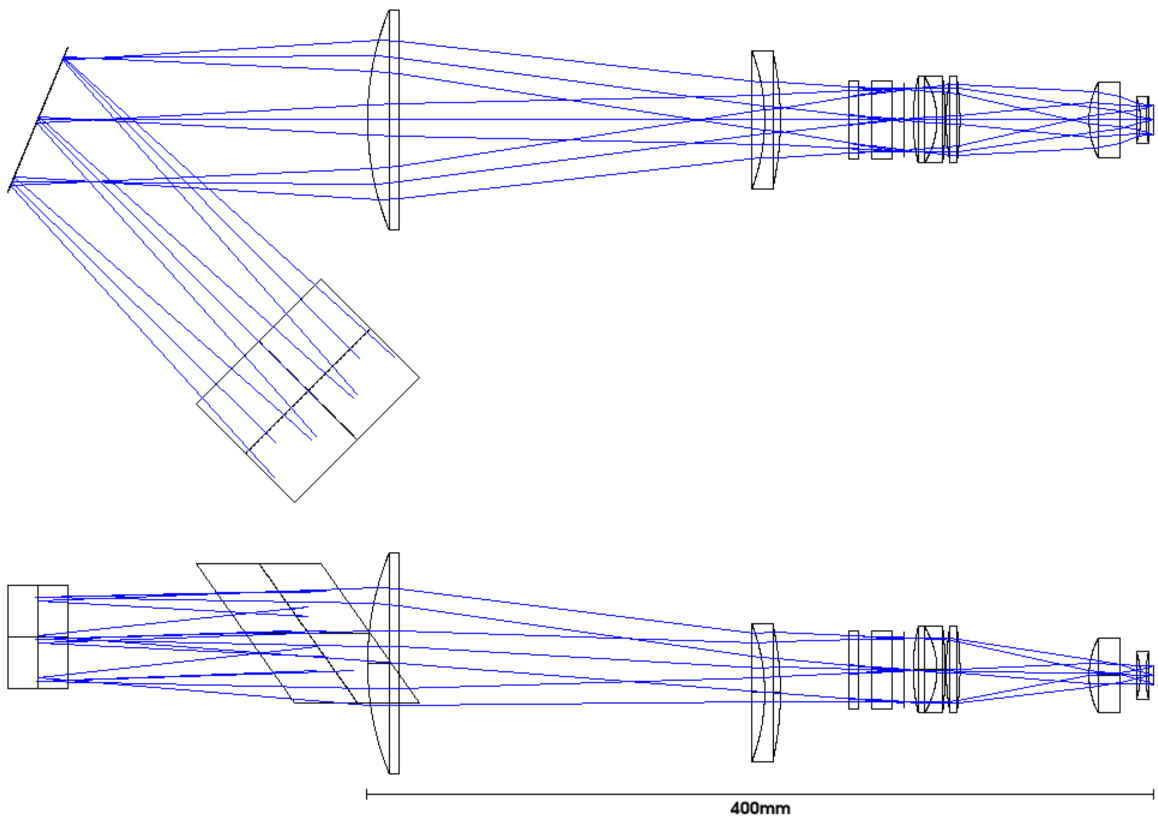

Figure 4: Top and side view of the optical layout of the focal reducer guider, including pick-up and folding mirrors. After the two elements of the collimator, a bandpass filter and an optional focus pyramid are placed. Following that is a five element camera. Note the offset elements on the lower figure.

A polychromatic spot diagram is shown in figure 5, spanning the bandpass of the filter, 550 - 800nm. Twelve guide field positions are shown, from the axis of symmetry of the field, and out to one side.

The average spot FWHM is 2.6 pixels or 0”85. While this is a significant smearing of the image, it is adequate for guiding.

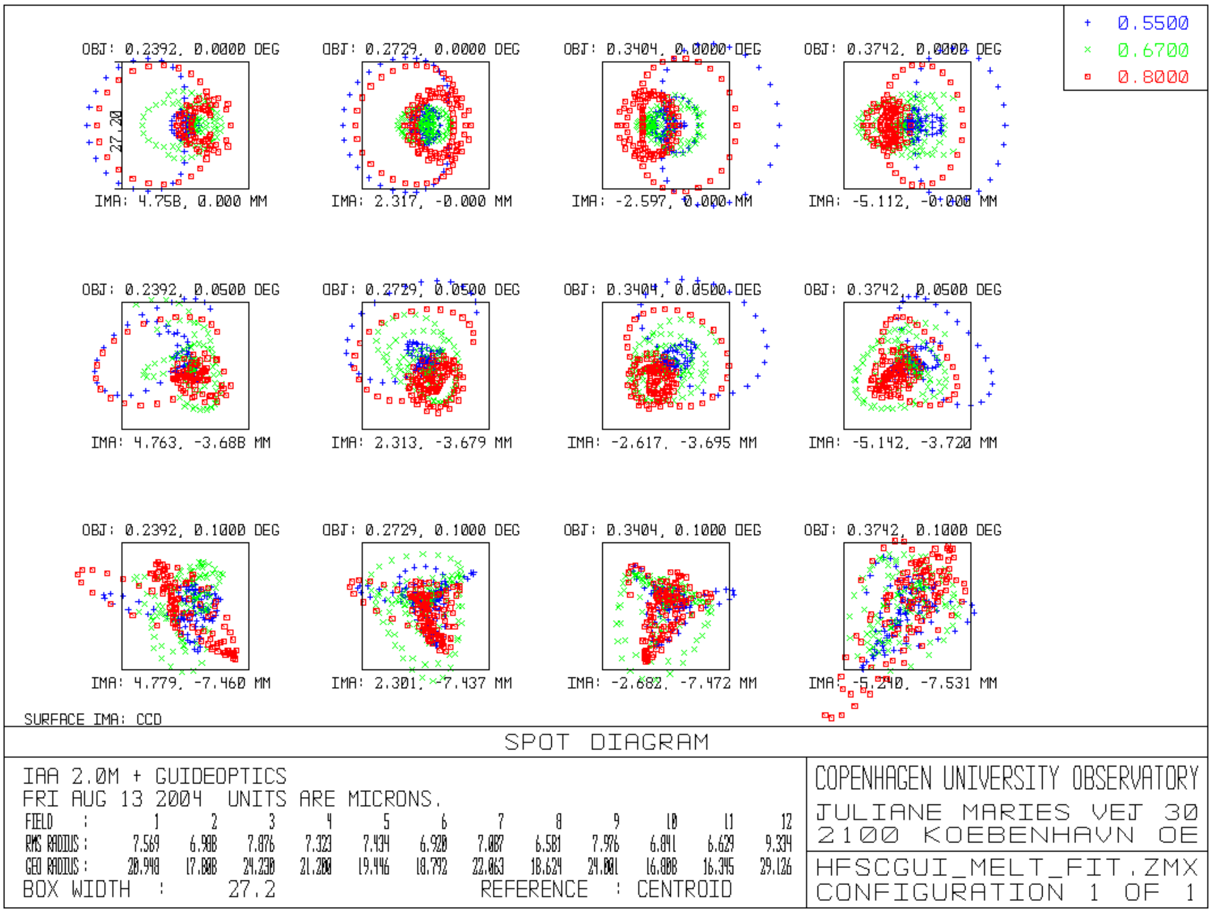

Figure 5: Polychromatic spot diagram for 12 field positions. Top row is on the axis of symmetry of the field, with leftmost being closest to the optial axis. Bottom right is the farmost corner of the guidefield. The side length of the square box corresponds to 4 pixels.

For complete specifications on the optical components, see appendix A.

6 Test results

6.1 Anti-reflection coating

All lenses of the autoguider were given a single-layer MgF_2 coating to optimise transmission. At the same time, test plate of 1mm BK7 was coated. The measured transmission of the test plate is shown in figure 6. A coating optimised for 700nm was requested, but the result seems to have optimal transmission around 750nm, with a somewhat degraded performance at 550nm.

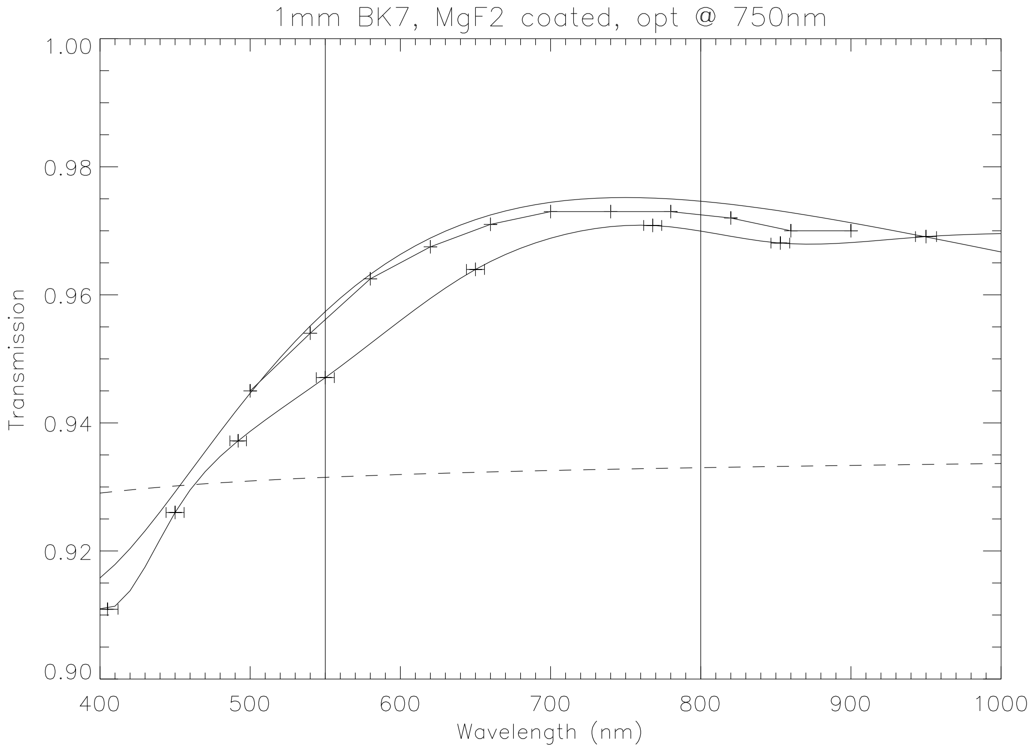

Figure 6: Verification of optics coating: Transmission through 1mm BK7, with single layer MgF_2 coating on both surfaces. Vertical lines marks the selected transmission range. Almost horisontal, dashed graph is the predicted transmission of uncoated BK7. Upper, unmarked graph is the predicted transmission for a coating optimised for 750nm. Graph marked with plusses is the transmission measured by the coating manufacturer. Graph marked with horisontal bars is the transmission measured at CUO.

6.2 Filter transmission

The 550nm - 800nm bandpass filter is made as a sandwich of OG530 glass for blue rejection and a Melles-Griot interference filter 03SWP620 for red cut-off. After glueing of the components, a coarse verification of the bandpass was made. The measurements are shown in figure 7, along with the predicted transmission. Unfortunately, a 5% light leak in the measurement setup was not eliminated. Taking this into account, the measurements are in agreement with the filter data.

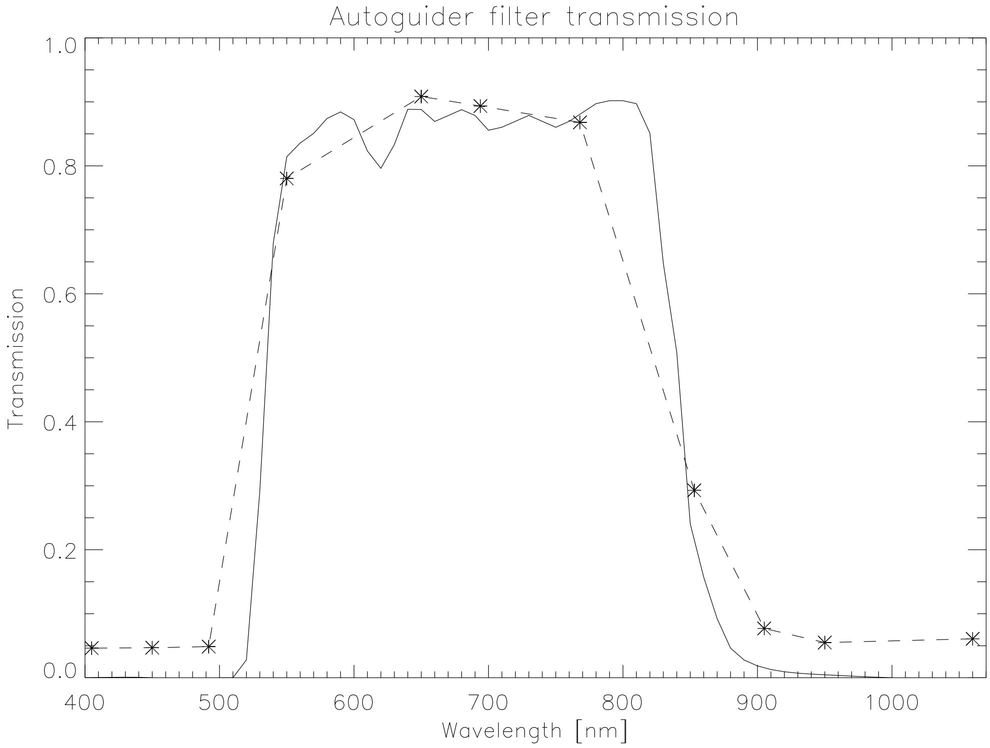

Figure 7: The fully drawn graph show the predicted transmission of the filter. The stars connected by a dotted line show a crude measurement of the filter transmission. The 5% transmission outside the bandpass is a measurement error.

6.3 Flexure

Gravitational strain on the autoguider will depend on telescope pointing, and guide star image displacement due to this effect must be small enough to avoid long exposure degradation. A reasonable limit for the allowable flexure can be chosen as no more than 0.1 arcsecond offset during a one-hour exposure. During an hour, the telescope will change the attitude by at most 15 degrees.

Flexure was tested by placing the autoguider on a table that can be tilted equivalently to altitude and rotator angle on an alt-az telescope. A LED-artificial star was placed in the focal plane. In this way, only the refractive elements are tested and the two mirrors of the autoguider are not included in the test.

As displayed in figure 8, a test of zenith distance (ZD) dependence was performed at selected rotator angles, and a full rotator revolution was tested at a zenith distance of 90 degrees. The 0 degree rotator angle is defined as the CCD front pointing up, and the rotation angle (RA) is measured counter-clockwise. The displacement in the vertical/Y direction on the detector was found to be several times stronger than X-movement, so X-coordinate data are not displayed.

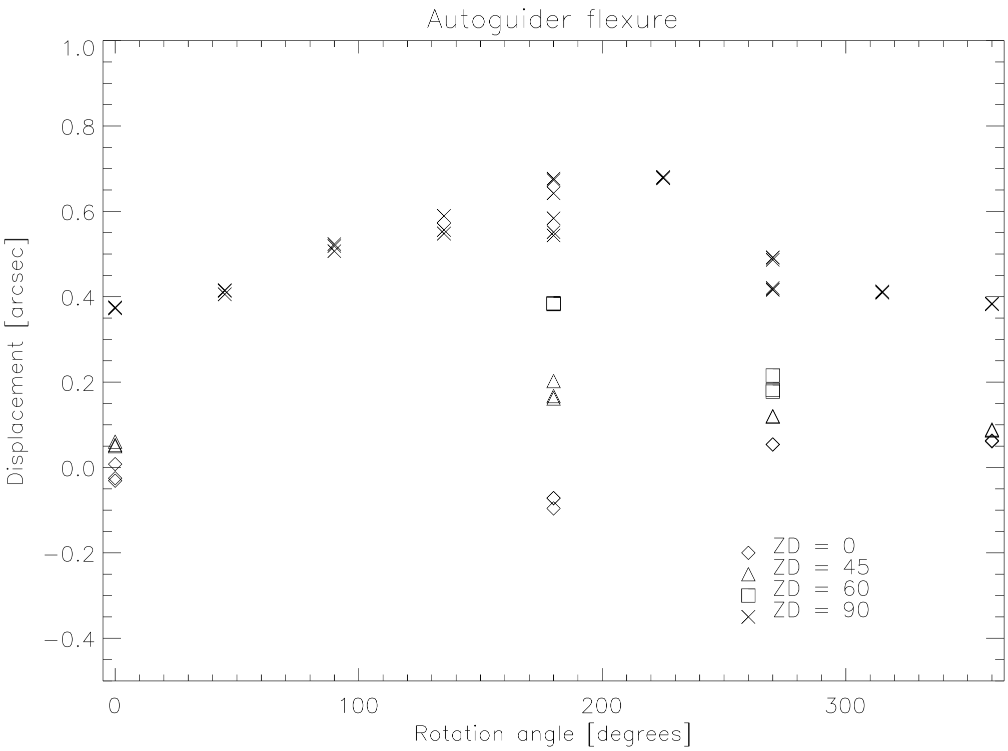

Figure 8: Autoguider flexure in the Y-direction on the detector, measured for a selection of rotation angles and Zenith distances.

From the figure, it can be seen that for ZD changes between 0 and 45 degrees, the position is very stable with the rotator position near 0 degrees, while at 180 degrees, the flexure is stronger. The 15 degree ZD change from ZD=45 to ZD=60 at RA=180 causes a 0.2 arcsec shift, and could perhaps be noticeable in science data. Near RA=0, the stability is again better, and for a ZD change from 45 to 90, the shift is only 0.3 arcsec.

The flexure tests were made with the focus pyramid in and out of the beam, with identical results. The focus signal of the pyramid was examined for attitude sensitivity, as is displayed in figure 9. No significant dependence is found.

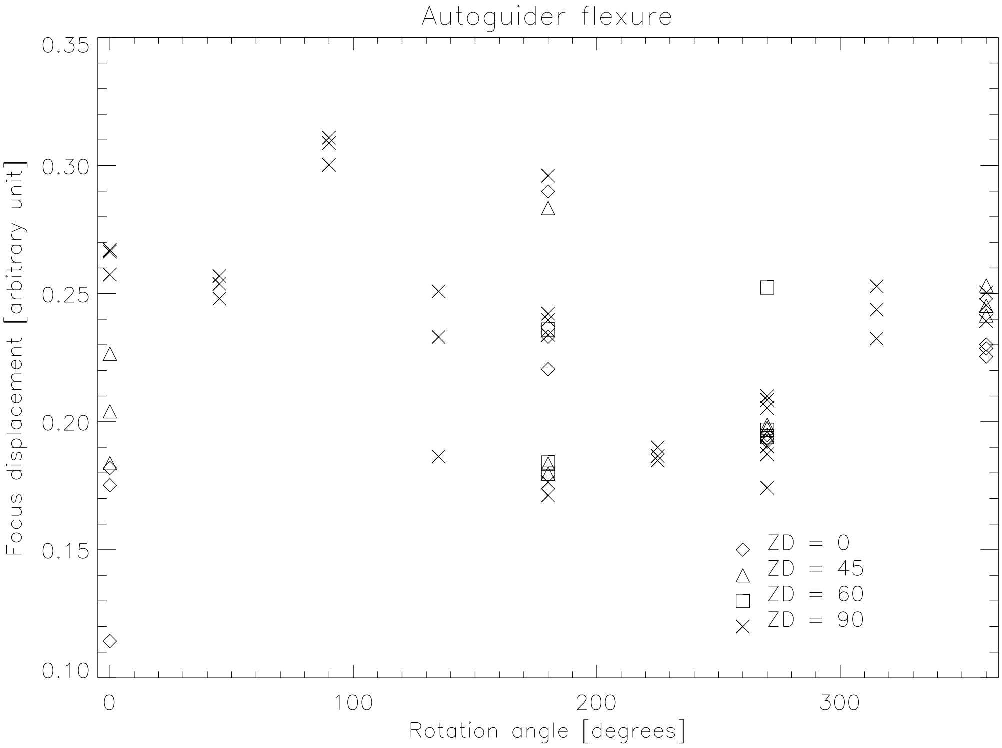

Figure 9: Focus pyramid signal as a function of Zenith distance and rotation angle. No significant dependence is found.

6.4 Environment requirements

In addition to the room temperature tests, testing was also performed at -15°C. After a slow cool-down, the integrity of the optics was verified and the moving parts of the pyramid wheel and shutter was found to work flawlessly. Some friction is present in the focus movement, but it does move. The control PC must be turned on at all times when the temperature is below 0°C - it cannot start up when cold, and the harddisk may be damaged if this is attempted. The electronics must at all times be kept free of condensation.

6.5 Focus pyramid

A sequence of images were obtained with the focus pyramid in the beam and a pinhole source at locations between ±2mm of the nominal focus. The positions of the four spots are plotted in the upper part of figure 10. Some deviation from symmetry is caused by the angles of the prism sections not being perfectly identical. Also note that the common centre of gravity moves with focus position. In the lower part of figure 10, the length of the two diagonals are shown versus the focus position. From this an in-focus diagonal of 27.85 pixels is read, with a sensitivity of 2.43 pixels/mm. This can be used as a starting point for the calibration on the telescope.

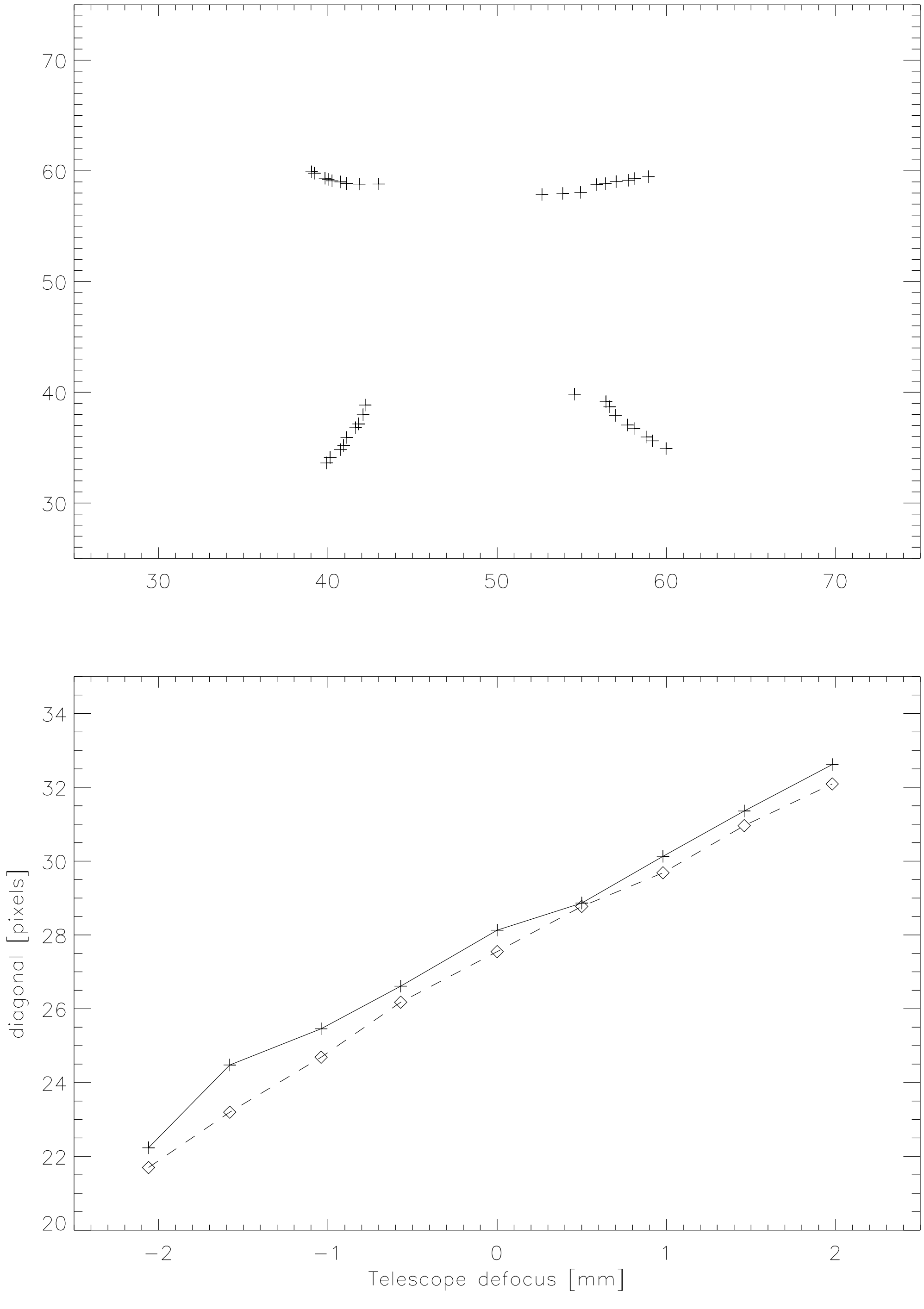

Figure 10: *top:* Location of the four spots created by the focus pyramid for different focus values. Scale is pixels. *bottom:* The relation between focus position and diagonal length in the quadrant.

6.6 Detector performance

The tests described here are all performed on the new CCD, replacing the one that failed during the first commissioning run.

The most critical performance parameters for the detector are quantum efficiency (QE), read-out noise (RON) and dark current.

6.6.1 Quantum efficiency

A measurement of the QE was performed when the CCD was already mounted behind the last lenses of the camera. The precision of the measurements was somewhat reduced for this reason, but still serves as a rough check of the sensitivity. The result is shown in figure 11, along with typical values provided by Kodak. For 550nm and 650nm, the measured QE is better than the Kodak numbers. The drop off at longer wavelengths is as expected also for this type of CCD.

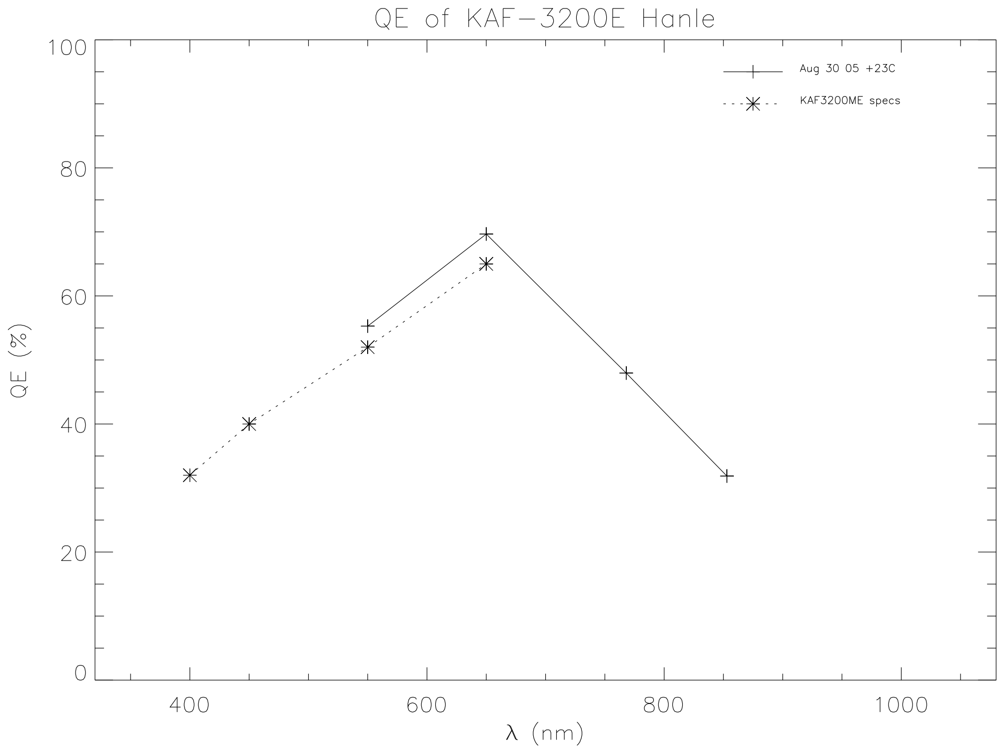

Figure 11: Quantum efficiency measured at four wavelengths, covering the transmission range of the autoguider filter. Also shown are four typical factory measurements.

6.6.2 Read-Out Noise, linearity and full well

RON and gain, the conversion factor between electrons and ADU, was determined from the noise statics of flat fields. A large number of illumination levels were examined by using various exposure times and by examining sections of flatfields that had illumination gradients. The result is shown in figure 12.

In the lower graph, the gain is plotted versus ADU. The overall level is constant, at a level of $1.1e^-$/ADU implying good linearity. At certain count levels, a deviating gain is measured. This is caused by imperfections in the analog-to-digital conversion. The CCD saturates at 42KADU, or $46Ke^-$, where charge blooming can be observed. The digital resolution is 16 bit, making digital saturation occur at 65KADU, above the CCD full well.

In the upper graph, RON is plotted versus ADU. The actual RON is estimated to $15e^-$, and the apparent increase with exposure level is attributed to other noise sources disturbing the measurement. As Kodak specifications are 7e$^-$ typical, 12e$^-$ maximum at -10°C, 1MHz, we apparently have not reached the true noise floor of the detector.

6.6.3 Dark current

An example of an exposure dominated by dark current signal is shown in figure 13. This is a 4 minute exposure with a detector temperature of 23°C. Above the average dark current level, a large number of "hot" pixels can be seen. Also emission from the read-out amplifier can be seen in one corner.

Dark current was determined by two methods: A simple level versus time measurement, and a linear fit to the vertical gradient in an image, from the additional dark current during the approx 28sec of full-frame readout. The level measurement resulted in a dark current of 6.4e$^-$/pixel/sec using the mean level, and 3.9e$^-$/pixel/sec when a median filter was used to eliminate the hot pixels. The gradient method yielded 7.0e$^-$/pixel/sec, all at 23°C. The measured dark current is below the typical values given by Kodak of about 9e$^-$/pixel/sec at 20°C.

The dark current is exponentially dependent on detector temperature with a doubling temperature of 6 - 7 degrees. The CCD temperature can be expected to settle at ambient temperature.

At 23°C, the dark current will build op signficantly during read-out of a full frame, so that even for a short exposure, the noise from dark current will be approximately as strong as the read-out noise. At lower temperatures, the dark current will rapidly decrease, making full frame exposures RON-limited. During guiding, the short read-out time of the small frames will assure that the performance is always RON-limited. However, one should be aware of the influence from isolated pixels with a much higher than average dark current.

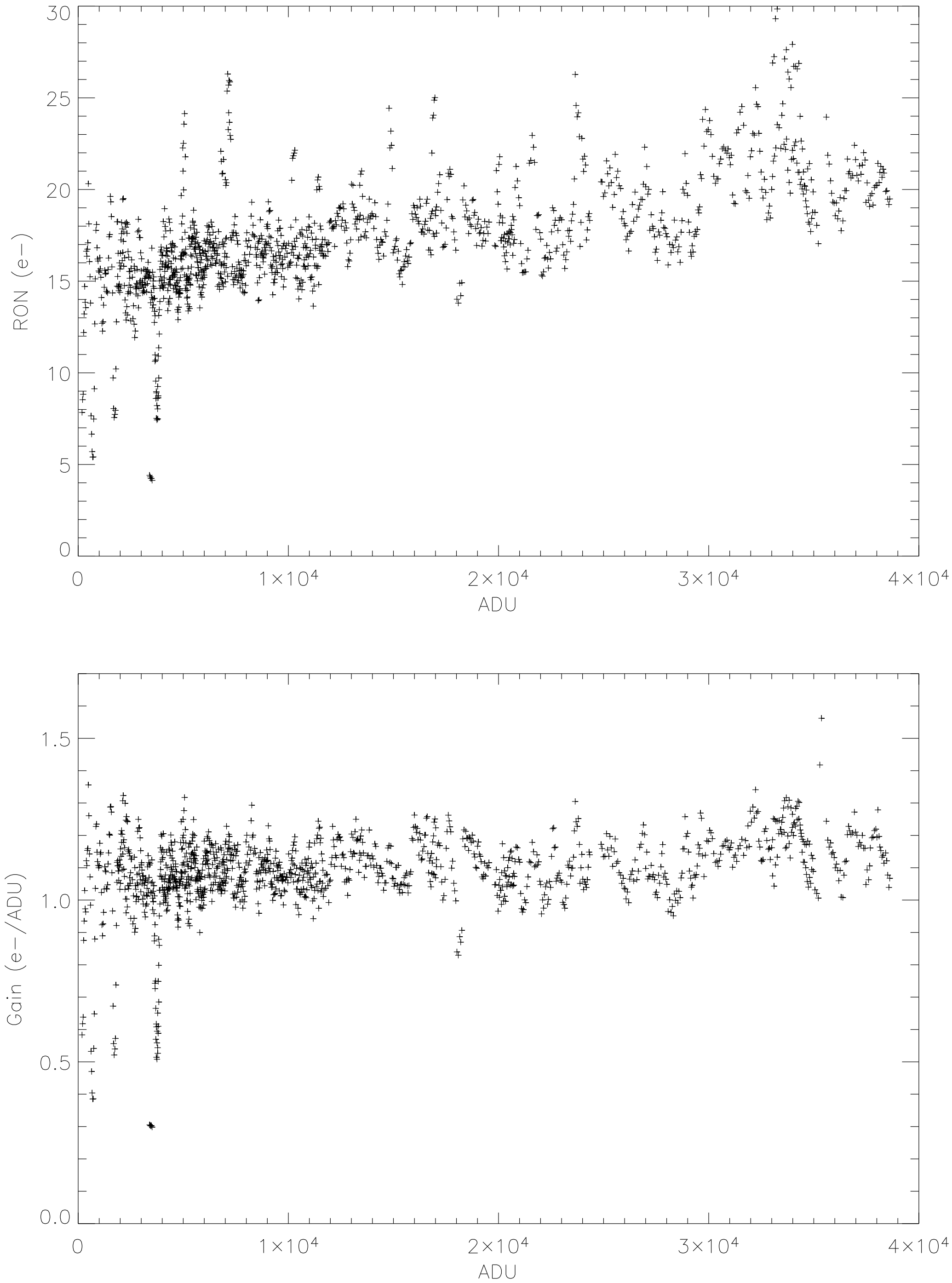

Figure 12: *top:* Measured read-out noise versus exposure level. *bottom:* Measured gain versus exposure level. Note the spikes from incorrect A/D conversion.

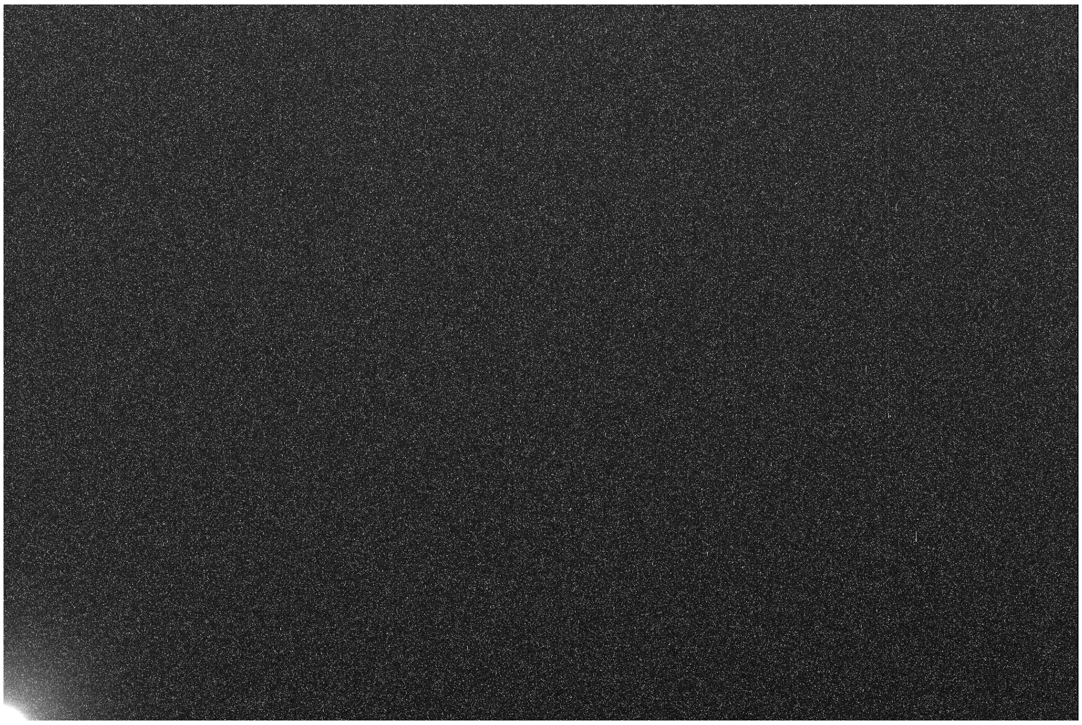

Figure 13: A full-frame 4 minute dark exposure, made at an ambient temperature of 23°C. Many hot pixels are visible, and the light from the amplifier can be seen in the lower left corner. A vertical gradient is faintly visible, due to the additional dark current during the 28 seconds of read-out.

A Optics parameters

In this appendix, abbreviated listings from the Zemax optical design program are shown.

GENERAL LENS DATA:

Surfaces	49
Stop	2
System Aperture	Entrance Pupil Diameter = 2010
Glass Catalogs	OPTIK-KONTOR
Ray Aiming	Off
Apodization	Uniform, factor = 0.00000E+000
Effective Focal Length	-4253.758 (in air at system temperature and pressure)
Effective Focal Length	-4253.758 (in image space)
Back Focal Length	4.281594
Total Track	4178.594
Image Space F/#	2.116297
Paraxial Working F/#	2.116297
Working F/#	2.078325
Image Space NA	0.2299315
Object Space NA	1.005e-007
Stop Radius	1005
Paraxial Image Height	28.75673
Paraxial Magnification	0
Entrance Pupil Diameter	2010
Entrance Pupil Position	2710
Exit Pupil Diameter	22.81541
Exit Pupil Position	-48.0026
Field Type	Angle in degrees
Maximum Field	0.3873314
Primary Wave	0.55
Lens Units	Millimeters
Angular Magnification	-88.09834

SURFACE DATA SUMMARY:

Surf	Type	Comment	Radius	Thickness	Glass	Diameter	Conic
OBJ	STANDARD		Infinity	Infinity		0	0
1	STANDARD		Infinity	2710		600	0
STO	STANDARD		-6926.3	-2694.243	MIRROR	2010	-1.021144
3	STANDARD		-1901.6	3619.167	MIRROR	480	-2.3505
4	COORDBRK		-	0		-	-
5	STANDARD	CUBE WALLS	Infinity	0		271.5979	0
6	STANDARD	195 PORT	Infinity	0		271.5979	0
7	STANDARD	M3 BASE	Infinity	0		271.5979	0
8	STANDARD	M3 PARK A	Infinity	0		271.5979	0
9	STANDARD	M3 CENTER	Infinity	0		271.5979	0
10	STANDARD	M3 PARK B	Infinity	0		271.5979	0
11	STANDARD	INNER WALLS	Infinity	0		271.5979	0
12	COORDBRK		-	0		-	-
13	STANDARD		Infinity	250		271.5979	0
14	STANDARD	CUBE BOTTOM	Infinity	-250		256.6055	0
15	STANDARD		Infinity	170		271.5979	0
16	COORDBRK		-	0		-	-
17	COORDBRK		-	0		-	-
18	STANDARD	DIAG MIRR	Infinity	0	MIRROR	118.1964	0
19	COORDBRK		-	0		-	-
20	COORDBRK		-	0		-	-
21	STANDARD	PRE FOC COMP.	Infinity	-195		261.4031	0
22	COORDBRK		-	0		-	-
23	COORDBRK		-	0		-	-
24	STANDARD	FOLD MIRR	Infinity	0	MIRROR	87.35364	0
25	COORDBRK		-	0		-	-
26	COORDBRK		-	0		-	-
27	STANDARD		Infinity	168.2		99.10888	0
28	STANDARD	COL1	149.979	16	N-SSK2	112	0
29	STANDARD		Infinity	186.25		112	0
30	COORDBRK		-	0		-	-
31	STANDARD	COL2	-98	8	N-SSK8	70	0
32	STANDARD		-161	62.8		70	0
33	COORDBRK		-	0		-	-
34	STANDARD		Infinity	-28		39.57134	0
35	STANDARD	FILTER	Infinity	5	N-BK7	40	0
36	STANDARD		Infinity	7		40	0
37	STANDARD	PYRAMID DUMMY	Infinity	10	N-BK7	40	0
38	STANDARD		Infinity	10.95		40	0
39	STANDARD	CAMERA	98	12	N-FK5	44	0
40	STANDARD	LENS 4	-41.51	4.25	N-SF1	44	0
41	STANDARD		-180.164	0.5		44	0
42	STANDARD	LENS 5	123.32	7	N-BAK1	44	0
43	STANDARD		-149.97	65.82		44	0
44	COORDBRK		-	0		-	-
45	STANDARD	LENS 6	41.51	15.5	N-LASF31	38	0
46	STANDARD		Infinity	10.6		38	0
47	STANDARD	LENS 7	-36.061	2.8	N-SF1	24	0
48	STANDARD		51.54	4		24	0
IMA	STANDARD	CCD	Infinity			18.45748	0

SURFACE DATA DETAIL:

Surface 16	COORDBRK
Decenter X	93
Surface 18	STANDARD DIAG MIRR
Aperture	Rectangular Aperture
X Half Width	50
Y Half Width	45
Surface 20	COORDBRK
Decenter X	-93
Surface 23	COORDBRK
Decenter X	95
Surface 24	STANDARD FOLD MIRR
Aperture	Rectangular Aperture
X Half Width	26
Y Half Width	40
Surface 26	COORDBRK
Decenter X	13.4
Surface 30	COORDBRK
Decenter X	15
Surface 33	COORDBRK
Decenter X	-11.75
Surface 44	COORDBRK
Decenter X	3

References

[Allen 73] Allen, C. W. : **Astrophysical Quantities**, Third edition, 1973, The Athlone Press, University of London.

[TNG WWW] Telescopio Nazionale Galileo web site : **La Palma sky brightness**, http://www.tng.iac.es/info/LaPalmasky.html